



HAL
open science

Highly Emissive Biological Bilirubin Molecules: Shedding New Light on the Phototherapy Scheme

Ahmed El-Zohry, Valentin Diez-Cabanes, Mariachiara Pastore, Taha Ahmed,
Burkhard Zietz

► **To cite this version:**

Ahmed El-Zohry, Valentin Diez-Cabanes, Mariachiara Pastore, Taha Ahmed, Burkhard Zietz. Highly Emissive Biological Bilirubin Molecules: Shedding New Light on the Phototherapy Scheme. *Journal of Physical Chemistry B*, 2021, 125 (32), pp.9213-9222. 10.1021/acs.jpccb.1c05308 . hal-03419821

HAL Id: hal-03419821

<https://hal.science/hal-03419821>

Submitted on 8 Nov 2021

HAL is a multi-disciplinary open access archive for the deposit and dissemination of scientific research documents, whether they are published or not. The documents may come from teaching and research institutions in France or abroad, or from public or private research centers.

L'archive ouverte pluridisciplinaire **HAL**, est destinée au dépôt et à la diffusion de documents scientifiques de niveau recherche, publiés ou non, émanant des établissements d'enseignement et de recherche français ou étrangers, des laboratoires publics ou privés.



Distributed under a Creative Commons Attribution 4.0 International License

Highly Emissive Biological Bilirubin Molecules: Shedding new light on the Phototherapy Scheme

Ahmed M. El-Zohry,^{a,b,*} Valentin Diez Cabanes,^c Mariachiara Pastore,^{*c} Taha Ahmed,^a and Burkhard Zietz^a

^a Department of Chemistry - Ångström Laboratories, Box 523, SE-75120 Uppsala, Sweden,

^b Department of Physics - AlbaNova Universitetscentrum, Stockholm University, SE-10691 Stockholm, Sweden.

^c Université de Lorraine & CNRS, Laboratoire de Physique et Chimie Théoriques (LPCT), F-54000, Nancy, France

* ahmed.elzohry@fysik.su.se, amfzohry@yahoo.com, mariachiara.pastore@univ-lorraine.fr

Abstract

Bilirubin (BR) is the main end-product of the hemoglobin catabolism. For decades, its photophysics were mainly discussed in terms of ultrafast deactivation of the excited state in solution, where, indeed, BR shows a very low green emission quantum yield (EQY), 0.03%, resulting from an efficient non-radiative isomerization process. Herein, we present, for the first time, unique and exceptional photophysical properties of solid-state BR, which change by changing the type of crystal, from a closely packed α crystal to an amorphous loosely packed β crystal. BR α crystals show a very bright red emission with an EQY of ca. 24%, whereas β crystals present in addition a low green EQY of ca. 0.5%. By combining Density Functional Theory (DFT) calculations and time resolved emission spectroscopy, we trace back this dual emission to the presence of two type of BR molecules in the crystal: a “stiff” monomer, M1, distorted by particularly strong internal H-bonds, and a “floppy” monomer, M2, having a structure close to that of BR in solution. We assign the red strong emission of BR crystals to M1 present in both the α and β crystals, while the low green emission, only present in the amorphous (β) crystal, is interpreted as M2 emission. Efficient energy transfer processes from M2 to M1 in the closely packed α crystal are invoked to explain the absence of the green component in its emission spectrum. Interestingly, these unique photophysical properties of BR remain in polar solvent like water. Based on these unprecedented findings, we propose a new model for the phototherapy scheme of BR inside the human body and highlight the usefulness of BR as strong biological fluorescent probe.

Introduction

Bilirubin IX α (termed BR hereafter) is among important biological metabolite, which undergoes biologically relevant processes through interaction with light, such as rhodopsin (causing vision)^{1, 2} and chlorophyll (photosynthesis in plants)³. BR is formed mainly from the degradation cycle of hemoglobin, and is naturally excreted with the help of liver, after binding to Human-Serum-Albumin (HSA) and other sugar groups.⁴⁻⁶ In newborns, however, the liver might not be active for few days after delivery, causing an accumulation of neurotoxic BR, which manifests itself as neonatal jaundice, affects the brain functionality, and leads to death in extreme cases. There is, thus, an urgent necessity to remove the accumulated BR. This is commonly done by resorting to BR phototherapy, that is by exposing the patient to irradiation in the visible range.⁷ The current established mechanism for BR excretion is that blue-to-green light converts the insoluble BR isomers, through isomerization process, into soluble ones that can be excreted.⁸ BR is a highly non-polar molecule that tends to interact with lipids rather than with physiological water molecules.⁹ Despite several studies about the photo-dynamics of BR, many processes are not well understood yet, due to the complexity of the BR chemical structure.¹⁰⁻¹⁴

Due to the insolubility of BR in most solvents, the photophysical properties of BR in vitro, or upon interaction with HAS, have been studied mainly in nonpolar or basic mediums to make clear solutions of BR, i.e. soluble form of BR.¹⁵⁻¹⁸ These photophysical studies indicate that upon photoexcitation an efficient ultrafast isomerization takes place converting the Z,Z-BR isomer into a mixture of Z,E isomers with a reaction quantum yield of 10%, while the rest retain back to the Z,Z-BR isomer.^{10, 12, 19} In CHCl₃, BR shows a very weak emission quantum yield (EQY) of 0.03% ($\tau_{\text{obs}} \sim 0.3$ ps, $\tau_r \sim 1.0$ ns), which increases to 0.3 % upon binding to HAS that restricts the dominating isomerization process of soluble BR.^{12, 20}

Despite the importance of the previous studies, we think this is not the best way to get biologically relevant insights into the BR photophysics, as it is not really connected to the expected behavior of BR molecules in the human-body or mammals in general, in which water is the main physiological medium. Simultaneously, due to the inactivity of the liver in the early days of the newborn, BR is expected to be present as small solid particles or as suspensions in the human body, especially if not bound to the HSA. This highlights the importance of studying BR in solid form or as suspensions in solvents like water to fully understand the reaction pathways of suspended BR particles before excretion under physiological conditions.

Unfortunately, to date, there is no such photophysical study on the BR in the solid state, which is an important topic.

Herein, we report for the first time a photophysical study on the BR in the solid state, by combining first principles calculations and time-resolved emission spectroscopy. We reveal unique strong emission properties of the BR crystals, and we rationalize these peculiar features on the base of the crystal structure. These unprecedented findings have been extended as well to suspensions in polar solvents such as water. Understanding the behavior of BR in the solid state should provide information on the behavior of BR particles in the newborns before excretion, and on the overall picture of excited state dynamics of BR molecules inside human bodies under phototherapy procedure. Moreover, our data also disclose the potential of utilizing BR particles as strong luminescent biological probe under physiological conditions.

Results and Discussion

Figure 1a shows the chemical structure of BR, which consists of two almost equivalent units, that is the *endo* and *exo* forms of a dipyrinone chromophore, linked by a saturated CH₂ group. The two halves also form strong internal hydrogen bonds (H-bonds), that can be broken upon illumination through a fast isomerization process, making the isomerized BR vulnerable to interact with water and special proteins to be excreted easily through the bile.¹⁹ The most stable isomer form of BR is called *Z,Z*-BR that is insoluble in most solvents, including water, due to the strong internal hydrogen bonds.²¹

The crystal structure package, based on the previous XRD results of BR crystals²², shows that two different BR units are present, hereafter indicated as *M1* and *M2* (see **Figure 1b** and **Figure S1**). Despite both BR monomers may appear quite similar, one fragment of *M1* shows an internal strong H-bond between the O atoms, which is absent in the *M2* fragments, see right part of **Figure 1b**. This H-bond is very strong, close to be a real covalent bond, with a distance of 1.18 Å (see **Figure S1**). This strong H-bond is also expected to make *M1* monomers more restricted and less flexible towards any excited state large-scale motions, and more insoluble in various solvents with respect to *M2* monomers. Interestingly, DFT calculations performed on the X-ray structures of *M1* and *M2* disclose that the two highest occupied and lowest unoccupied molecular orbitals (HOMO-1/HOMO and LUMO/LUMO+1) are not-longer quasi-degenerate for *M1* (see **Figure 1c**). The structural distortion, indeed, engenders a sizeable stabilization (~ 0.9 eV) of the LUMO level, being localized on the distorted moiety (see left

part **Figure 1c**), and a slight destabilization of the HOMO level. Consequently, the calculated absorption spectrum (**Figure 2a** and **Table S2**) presents two distinct absorption peaks, centered around 390 and 490 nm, respectively, corresponding to local fragment excitation from the HOMOs to LUMO+1 (S_2) and to LUMO (S_1), respectively (see **Figure S3-4**). A single absorption band is, on the other hand, calculated for M2, around 385 nm, due to the near energy degeneracy of LUMO and LUMO + 1 (**Figure 1c**). Thus, the absorption spectrum of the crystal package of BR is expected to be a combination of M1 and M2 spectral bands. Note that the absorption features of the monomers are not substantially modified upon the interaction with the neighboring molecules of the crystal (see **Table S3**). We called this crystal package “ α crystals”. Interestingly, the simulated spectrum of BR in CHCl_3 , after full structural relaxation, exhibits one single absorption peak around 395 nm, very close to the calculated maximum absorption of M2 (see **Figure 1c** and **Figure 1a**), as expected on the basis of their similar geometrical and electronic properties (see section 2.1 in the SI). This indicates that M1 can only be identified in the solid state BR, where these strong H-bonds are formed due to the crystal packing.

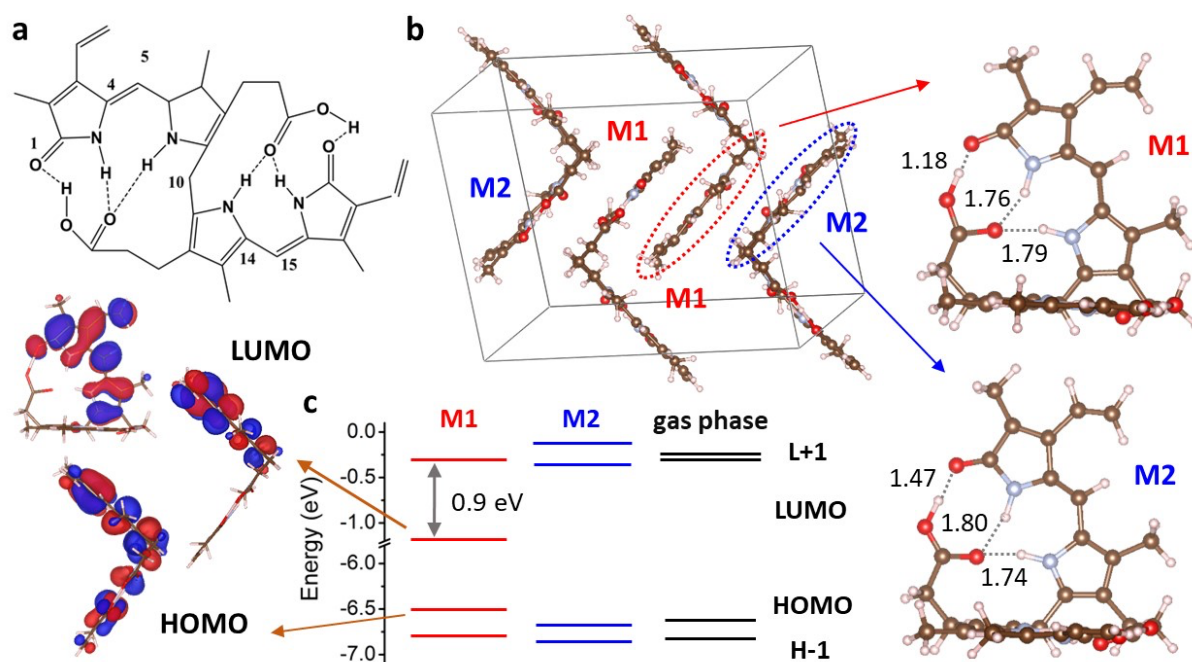


Figure 1: (a) Structure of Z,Z BR isomer, showing the internal hydrogen bonds. (b) Perspective view of the unit cell conforming the BR crystals made of two pairs of monomers (M1 and M2), which are displayed on the right part of the image. The H-bond distances highlighted here are given in Å. (c) Frontier energy levels for M1 (red), M2 (blue) and BR in gas phase (black), with the shapes of the LUMO and HOMO of M1 represented in the left part of the graph. The rest of the frontier orbital shapes are collected in Figure S3. The isovalue used to plot the isodensities was 0.02 a.u.

To verify these theoretical observations, absorption and emission of BR α crystals have been studied in crystalline solid form and after dissolution in CHCl_3 , see **Figure 2b**. Upon dissolving the BR crystals in CHCl_3 , it has been noticed that the solution is not fully clear and a simple filtration step is needed to have a clear solution. The filtered solution in CHCl_3 shows a strong absorption band centered at ca. 450 nm, with a corresponding weak emission band at 520 nm, matching with the previous measurements of BR in CHCl_3 .^{10-12, 14} However, the BR α crystals (see the SEM image for large crystals, **Figure 2c**) show a broader absorption band centered at ca. 475 nm, with a significant absorption tail extending into 750 nm (blue solid and dashed lines in **Figure 2b**). Interestingly, the absorption band of α crystals matches quite well with that of soluble BR in CHCl_3 (full and dashed black lines in **Figure 2b**) in the high-energy side of the spectrum. Surprisingly, the emission of α crystals shows a stronger red-shifted band centered at ca. 700 nm. To the best of our knowledge, this observation has not been detected previously for the BR molecules. However, based on our quantum chemical calculations, we can interpret these spectral differences between BR in CHCl_3 and BR at solid state as arising from the contribution of M1 monomers. While in the BR α crystals, indeed, both M1 and M2 forms are present, the filtered solution may not contain M1, due to its lower solubility caused by the strong intramolecular H-bond mentioned above. To indirectly verify this assumption, we dissolved BR α crystals in CHCl_3 , removed most of the clear solution, and re-evaporated the CHCl_3 , forming the BR crystals again. In this way, we expect to have less M2 monomers in the formed crystals, since most of them have been removed by dissolution in CHCl_3 . The BR crystals have been imaged using SEM before and after this rough re-crystallization process, see **Figure 2c and d**. Clearly, as shown from the SEM images, this re-crystallization process is not optimum, but still the crystallinity of the BR particles is present as shown by the XRD measurements, see **Figure 2e**. These new BR crystals are named “ β crystals”. As expected, the absorption and the emission properties of the two BR crystal forms are different, see **Figure 2b**. The absorption band of the β crystals resembles to that of the α crystals but a clear absorption peak at 500 nm is present. This low-energy absorption peak matches with the calculated lower-energy absorption band for the M1, localized on the “distorted” dipyrinone unit, see **Figure 2**. On the other side, the measured emission of the β crystals is slightly different. Despite the main emission peak at ca. 700 nm is still present, the emission is weaker, and there is the appearance of a new emission shoulder at roughly 525 nm. The position of this new emission shoulder interestingly almost coincides with the emission band of soluble BR in CHCl_3 , see **Figure 2b**.

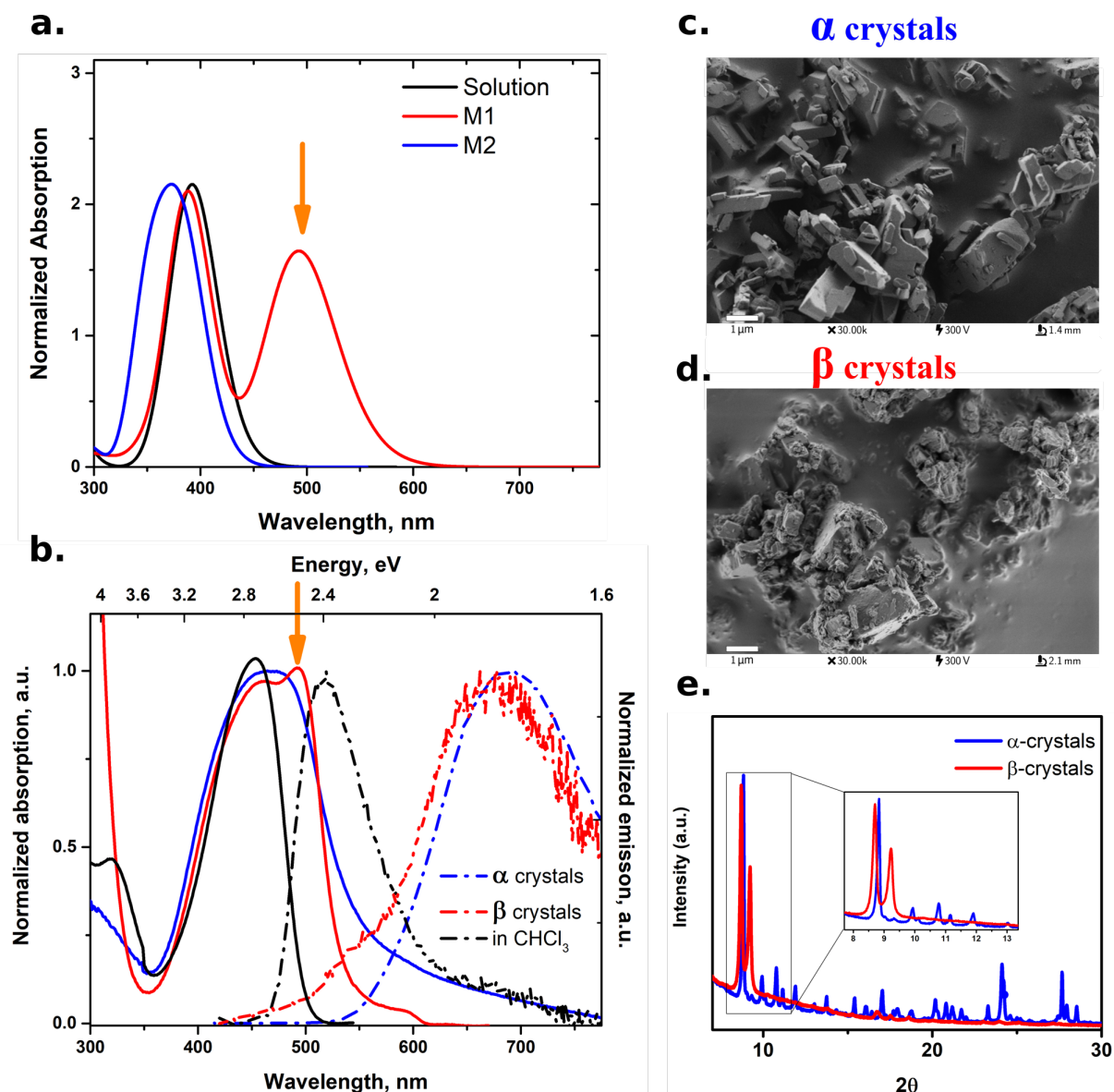


Figure 2: (a) Calculated absorption spectra for M1 and M2 monomers of bilirubin. The nature of the main transitions conforming these spectra are reported in Table S2. (b) Experimental absorption and emission of bilirubin in solution and solid state. SEM images for α crystals, M1 and M2 (c), β crystals mainly M1 (d). (e) XRD measurements for α crystals and β crystals of BR. The XRD data shows many isomers in the crystal package, most “M2” isomers have disappeared after rough recrystallizations, due to their solubility or their conversion to another isomer “check the new intense peak close the potential M1 peak”.

To fully rationalize these peculiar spectral properties, especially the emission ones, we utilized time-resolved emission with pico-second time-resolution. The BR α crystals show long-lived emission at room temperature with a corresponding emission lifetime of 240 ps, see **Figure 3a**. Knowing that EQY of BR in solution is about 0.03% (average emission lifetime is about 0.3 ps),^{12, 20} the EQY for the BR α crystals is about three orders of magnitude higher ($\sim 24\%$). This high EQY of BR α crystals is possibly due to the restrictions of ultrafast isomerization processes

of BR, which increase the barrier for the conical intersection in the excited state.¹⁰⁻¹² Moreover, we interpret this red-emission peak as coming from M1, whose S₁ state is lower in energy with respect to M2 (492 nm vs 384 nm for M1 and M2 respectively). We then report transient-emission data measured on the BR β crystals in **Figure 3b**. Firstly, the emission peak at ca. 700 nm has a shorter lifetime of 140 ps, possibly due to surface defects formed upon the recrystallization process.^{23, 24} Secondly, a clear short life-time emission shoulder at 525 nm is appearing, with an average lifetime of 5 ps (EQY ~0.5%), see **Table 1**. We assign this short emission peak, which coincides with the emission of BR in solution, to the M2 monomers emission, present in the β crystals. Interestingly, the EQY of M2 in β crystals is similar to the BR upon binding to HSA, indicating that the isomerization of M2 in β crystals is partially restricted.^{12, 20} The question that we need to answer now is why the green emission shoulder is not appearing in the well packed α crystals. To validate our assignments and explain the differences in the emission dynamics, we have explored the possibility of realizing Förster Resonance Energy Transfer (FRET) from M2 to M1 among the very close and well packed different BR molecules in the α-crystals (see details in section 1.6 in SI). Invoking a FRET mechanism herein is not exotic, since, previously, FRET was also suggested to occur between the two halves of BR (XBRs) in solution, then disappearing in the XBR molecule and upon deprotonation of BR.¹⁰

FRET rates are, indeed, dependent of the relative position of the donor acceptor pairs, being expressed as

$$k_F = \frac{1}{\tau_0} \frac{R_0^6}{|r_A - r_D|^6}, \quad (1)$$

where τ_0 is the lifetime of the donor excited state, R_0 is the Förster radius, r_D and r_A are the position vectors of the donor (M2) and the acceptor (M1) respectively. The Förster radius, defined as the distance between the donor and the acceptor when the FRET has 50% probability, can be calculated from the donor luminescence efficiency, the overlap integral of the donor emission spectrum and the acceptor absorption spectrum, and the dimensionless orientation factor κ^2 , which can vary from 0 to 4 (see Supporting Information for more details). The calculated κ^2 values for the four possible combination of neighboring M2-M1 pairs present in the crystalline structure (see **Figure S5** and **Table S4**) amount to 0.07, 0.86, 0.78 and 2.2. This result manifests an anisotropic transport, with one of the donor-acceptor pair energy transfer being clearly unfavorable with respect to the others. Notably, these values of κ^2 yield to

donor/acceptor pair Förster radii of 10.2, 15.6, 15.4 and 18.3 Å, being of the same order of magnitude of the FRET radii estimated in common energy transfer processes occurring in biological systems (i.e. R_0 values for naphthalene–dansyl pairs amounted to 23.3 Å).²⁵ These results, thus, corroborate the hypothesis that long range energy transfer processes may take place among neighboring M2 and M1 monomers in the α crystals arrangement. The FRET process is also confirmed through the decay associated spectra (DAS) obtained by fitting the time-resolved data, as shown in **Figure 3 c-d**. For the α crystals, two emission lifetimes are needed for the global fitting, a short lifetime of 25 ps and a longer lifetime of 240 ps. The DAS for the latter shows an emission like behavior as expected. On the other hand, the DAS for the short lifetime component shows a positive signal around 570 nm and a negative part centered at 715 nm. This negative part is an indication for the FRET process between the emission components at the blue side (M2) to the ones at the red side (M1) of α crystals through the absorption of M1 monomers.²⁶⁻²⁸ The ratio between the positive and the negative part of DAS for 25 ps component indicates that the FRET efficiency is at least 60-70%. For the β crystals, the DAS of the short component (~5 ps) shows only an intense positive part extending to 675 nm, indicating the absence of FRET process between the blue and red emission sides. We thus expect that upon the performed recrystallization, the ordered crystalline packing is broken down; hindering efficient FRET processes between M2 and M1, thus making M2 emission at ~525 nm appearing.

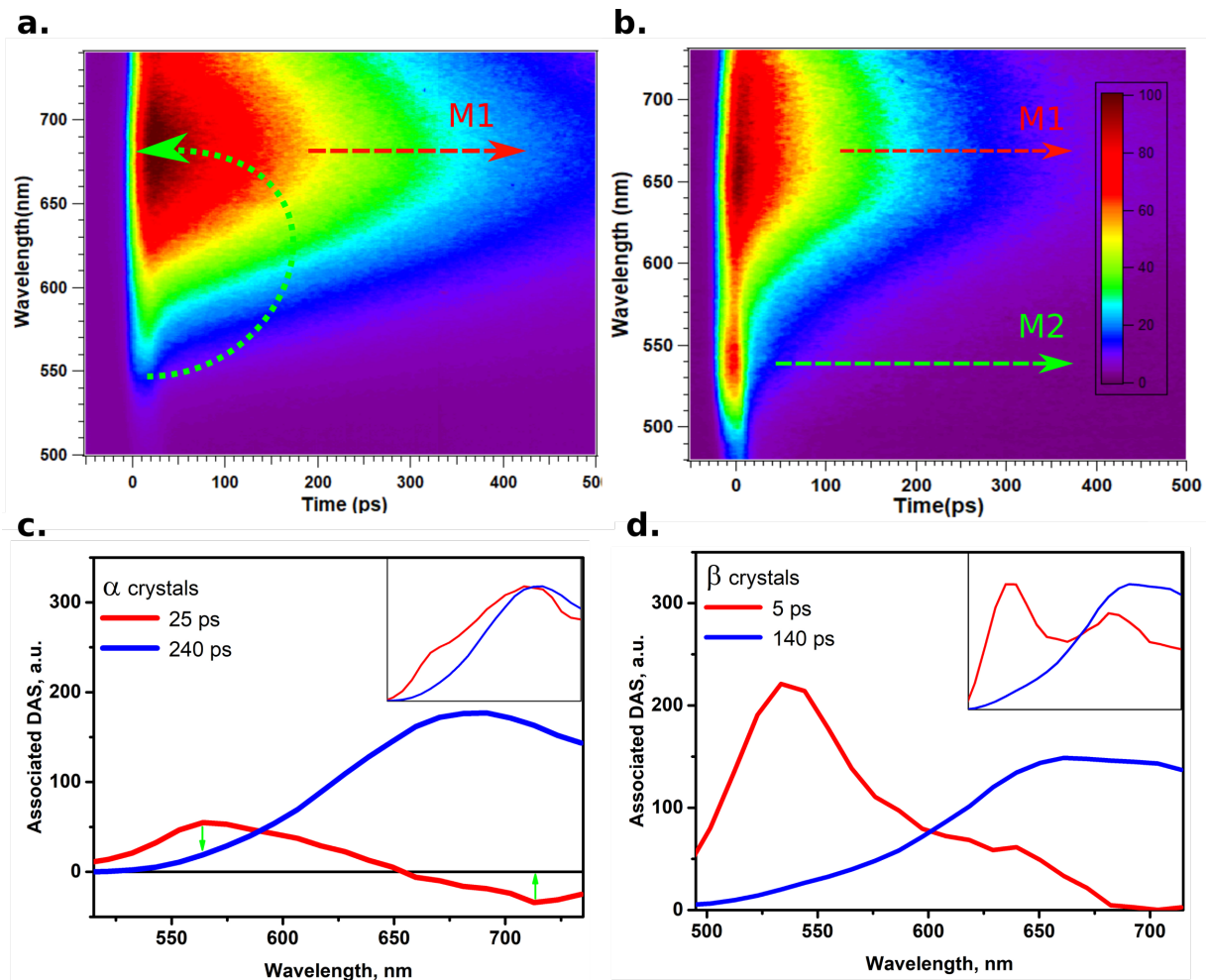


Figure 3: a) Time-resolved emission properties of bilirubin crystals. b) Time-resolved emission of recrystallized BR particles. c) Decay associated spectra for α crystals for two emission lifetimes. In the inset the extracted normalized emission spectra at corresponding times 25 ps (red) and 240 ps (blue). d) Decay associated spectra for β crystals for two emission lifetimes. In the inset the extracted normalized emission spectra at corresponding times 5 ps (red) and 140 ps (blue). See text for more information.

Table 1: Extracted emission lifetimes of bilirubin under various conditions using global fitting procedure.

Environment	@ 550 nm / ps	@ 700 nm / ps
MeCN	4.3 ± 0.1	260 ± 4
MeOH	3.1 ± 0.2	250 ± 15
Water	5 ± 1.1	265 ± 5
α crystals	25 ± 2.8	240 ± 10
β crystals	5 ± 1	140 ± 6

To determine the amount of active non-radiative channels, the emission of BR crystals has been measured at low temperature (77 K), and, as it is apparent in **Figure 4a**, the emission intensity increases by a factor of 3, meaning that the emission QY can reach $\sim 75\%$. This indicates that

non-radiative decay channels are still active at room temperature for the α crystal, suggesting a residual activity of large scale motions,^{20, 29-34} aggregation effects^{32, 35, 36}, or heat dissipation by crystal phonons.^{37, 38}

To correlate the behavior of BR in the crystal form and the one in the physiological environment, we performed emission measurements for suspensions of BR crystals in water, and other polar solvents such as MeOH and MeCN, see **Figure 4b**. All the emission data show results consistent with those measured of the solid phase, indicating that the photophysical properties of BR inside the human body can be rather safely interpreted on the basis of these results. Interestingly, there is also a conversion process between the insoluble M1 to soluble M2 monomers upon changing basicity of the environment, or inducing a thermal effect. Adding small volumes of an organic base (Et_3N) to the suspensions of BR in MeCN shows a systematic suppression of the red-shifted emission, and an evolution toward the well-known green emission of BR in solution. Such an effect of equilibrium between M2 and M1 monomers depends on the solvent as well as on the strength of the employed base, as shown in **Figure S6 in SI**. This is the consequence of the rupture of the strong H-bonds in M1 and the formation of soluble M2 monomers in solution. Similarly, by rising the temperature of the suspended BR crystals in MeCN, the red emission from M1 monomers decreases, while the green emission of M2 monomers increases. Moreover, this thermal effect is not reversible, thus cooling down the suspensions again to room temperature does not regain the red emission due the breakdown of the H-bonds and the loss of the symmetry of the crystal packing, see **Figure 4d**.

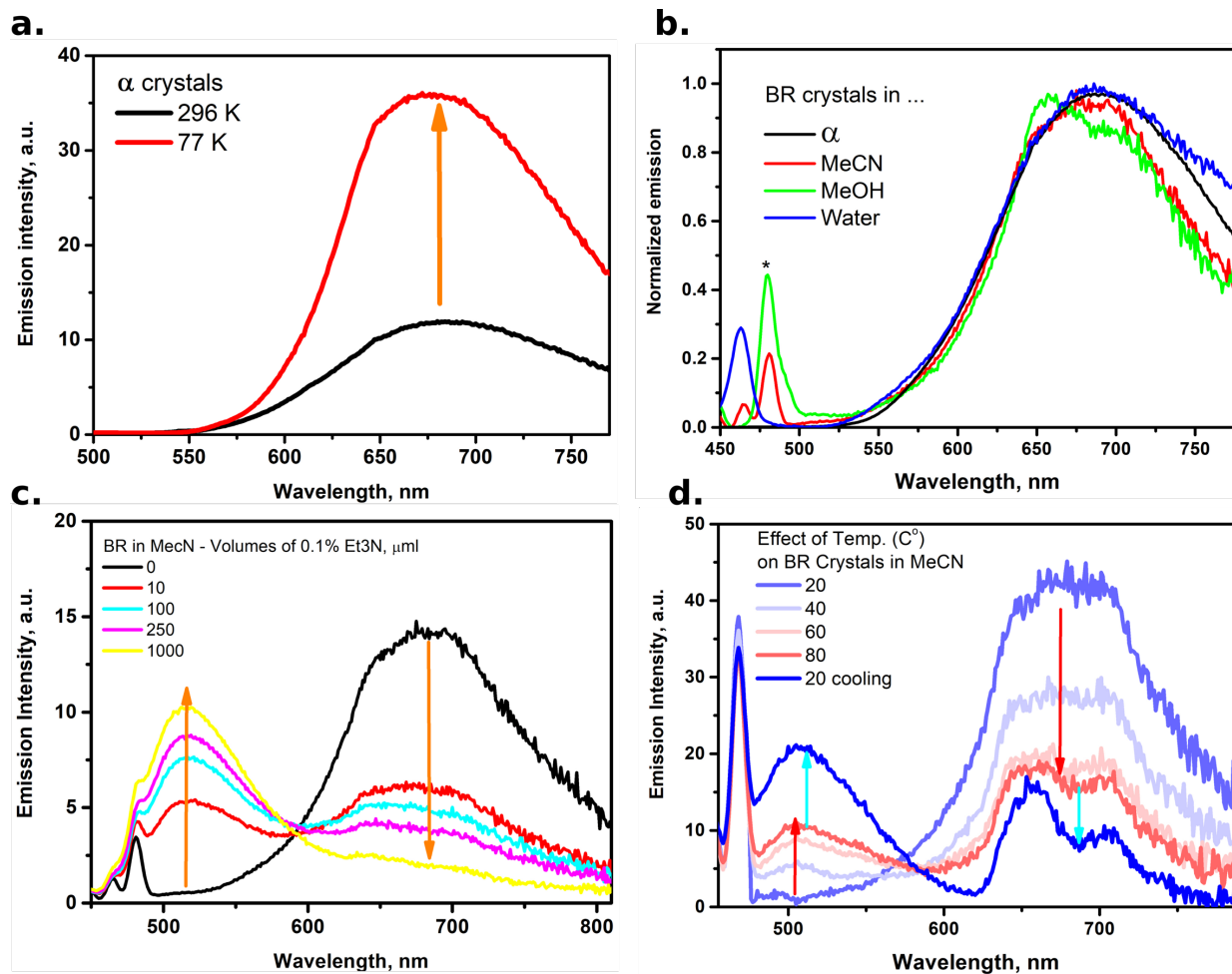
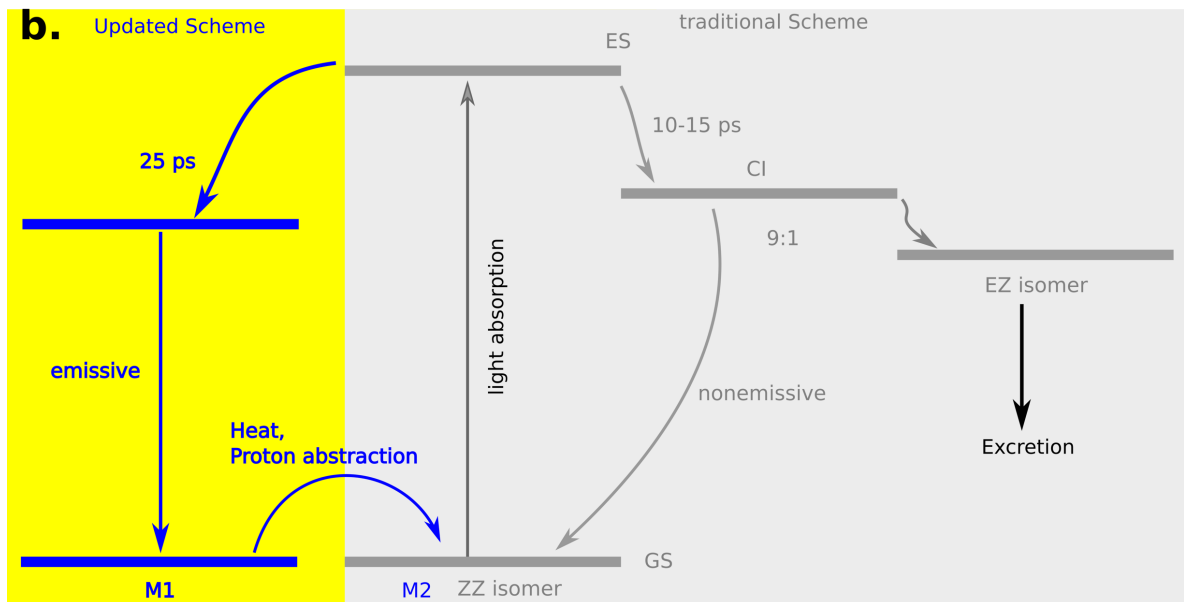
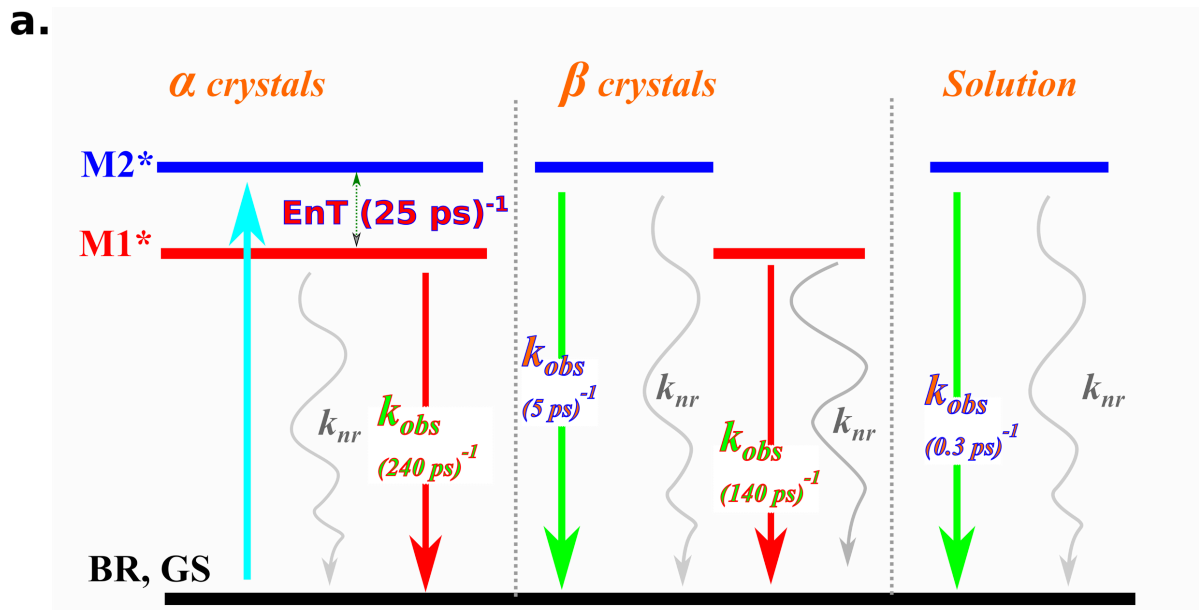


Figure 4: a) Effect of reducing the temperature on emission properties of α crystals. b) Emission spectra of suspended BR crystals in various solvents as shown in the legend. The star shows the Raman lines of solvents. c) Addition of organic base Et₃N to the suspension of BR crystals in MeCN. d) Effect of heating and cooling the suspensions of BR in MeCN. See text for more information.



Scheme 1: (a) Schematic representation for the possible photophysical processes in solid state crystals of bilirubin. (b) Schematic representation for the old and the updated view for the photoexcited state of BR upon interaction with the incident light in the human body.

Scheme 1a summarizes the current photophysical findings for BR under three different phases. In the well-packed crystals, α crystals, BR is present in the form of M1 and M2 monomers, having different, geometries, relaxed energies, and electronic properties. Upon light absorption, an efficient FRET process, with a lifetime of ~ 25 ps, occurs from M2 to M1, making M1 the responsible for the main red-shifted emission at 700 nm with a QY close to 24% (τ_{obs} 240 ps). For the loosely packed β crystals, the energy transfer is hindered and a dual emission, at ~ 525 nm ($\tau_{\text{obs}} \sim 5$ ps) and at ~ 700 nm ($\tau_{\text{obs}} \sim 140$ ps), is measured. When BR is completely soluble, M1 monomers are insoluble due to the strong H-bonds, only emission at 525 nm can be

observed from soluble M2 monomers, with an emission QY of 0.03% (τ_{obs} 0.3 ps) due to the well-known isomerization process. Apparently, the isomerization process and, possibly, other non-radiative deactivation processes are still efficient in the solid state, since the BR crystal emission QY cannot reach to unity even at low temperature (see **Figure 5a**). Moreover, in suspensions, by changing the temperature or controlling the environment basicity, one can break the strong intramolecular H-bond characterizing M1, thus obtaining symmetrical M2 monomers and controlling the emission properties.

Despite the effectiveness of the phototherapy to treat excess levels of BR,^{8, 39} these present findings may shed a new light on the current understandings for the phototherapy for excretion of BR. Previously, no significant efficiency differences have been detected upon using blue light (~ 460 nm) or green light (~ 500 nm).⁴⁰ As mentioned before, all the previous studies about BR focused on the BR in solution, that is on the “M2” monomer in our scheme, and this leads to the picture about the current mechanism, reported in **Scheme 2b**, for interaction of M2 with incident light. In that picture, M2 reaches the conical intersection (CI) within 10-15 ps, then isomers of different ratio 9:1 (ZZ:EZ) are formed.^{41, 42} Inserting M1 monomers into the same picture opens another deactivation channel (FRET to M1) for the excited M2 monomers, thus reducing the efficiency to form excretable EZ isomers. Since M1 monomers are highly hydrophobic, thus absorption of light by M1 monomers is expected to be useless rather than the expected red emission, which might provide the jaundice colour for infants. As we have shown, M1 can be converted into excretable M2 monomers by the heating due to the incident light or proton abstraction by some proteins. These are, however, expected to be slow processes, ~hours to days, thus requiring prolonged exposure to irradiation, with the correlated higher risks for newborn’s health, as it is the case in the current phototherapy protocol. (can we cite some papers on the cancer risk of phototherapy?) Further investigations in vivo are, however, needed to confirm these hypothesis.

Conclusion

Despite the biological relevance of BR and the understandable great interest devoted to characterize its photophysics in the past years, previous works have only addressed its absorption and emission properties in solution, which, however, does not mimic the actual biological environment, where BR is likely to be present as small solid particles or as suspensions when not bound to the HAS. Here, we have shown for the first time that BR single crystals present a unique and completely different photophysical behavior with respect to that

reported in the literature. Analysis of the BR crystal (α -crystals) structure and quantum chemical calculations discloses that in the solid-state phase, BR is present in two different monomeric units, namely M1 and M2. Particularly, strong internal hydrogen bonds make M1 very poor soluble and slightly distorted in the crystal packing with respect to M2 and to the BR structure in solution. This structural distortion leads to a sizeable stabilization of the lowest unoccupied energy levels in M1 and, thus, to a marked shift at longer wavelengths of both absorption and emission, occurring at ca. 700 nm with a high emission QY of ca. 24%. When dissolving BR α crystals, the more soluble M2 molecules are dissolved, and after irradiation of the filtered solution the well-known and efficient isomerization process reduces the emission QY to 0.03%. We also obtained different BR crystals (β crystals), mainly composed of the less soluble M1 units, after dissolution of α -crystals in CHCl_3 , elimination of most of the clear solution and solvent re-evaporation. The different crystal forms have striking different photophysics that we have shown, based on theoretical calculations, originate from the possibility of realizing efficient long range energy transfer (FRET) processes from M2 to M1 in the original α crystals, leading solely to the emission at 700 nm. Inefficient FRET in β crystals gives rise to dual emission, at ca. 525 and 700 nm, from M2 and M1 respectively. Similar photophysical properties have been detected for BR particles in water as a physiological environment, suggesting that the observed photophysical properties in solid state can also occur under the phototherapy procedure. We thus suggest a more complex phototherapy scheme of BR, which may explain the prolonged exposition to light irradiation required to have an effective treatment. Therefore, our study opens new dimension for understanding the BR excited state dynamics for an efficient phototherapy, and the possibility of utilizing BR as a biological fluorescent probe. ?

References

1. Polli, D.; Altoe, P.; Weingart, O.; Spillane, K. M.; Manzoni, C.; Brida, D.; Tomasello, G.; Orlandi, G.; Kukura, P.; Mathies, R. A.; Garavelli, M.; Cerullo, G. *Nature* **2010**, 467, (7314), 440-443.
2. Broser, M.; Spreen, A.; Konold, P. E.; Peter, E.; Adam, S.; Borin, V.; Schapiro, I.; Seifert, R.; Kennis, J. T.; Sierra, Y. A. B. *J. N. c.* **2020**, 11, (1), 1-10.
3. Kato, K.; Shinoda, T.; Nagao, R.; Akimoto, S.; Suzuki, T.; Dohmae, N.; Chen, M.; Allakhverdiev, S. I.; Shen, J.-R.; Akita, F. *J. N. c.* **2020**, 11, (1), 1-10.
4. Dosch, A. R.; Imagawa, D. K.; Jutric, Z. *Surg Clin N Am* **2019**, 99, (2), 215-+.
5. McDonagh, A. F.; Palma, L. A.; Lightner, D. A. *J. S.* **1980**, 208, (4440), 145-151.
6. McDonagh, A. F.; Lightner, D. A. *J. P.* **1985**, 75, (3), 443-455.
7. Stokowski, L. A. *Adv. Neonatal Care* **2011**, 11, S10-S21.

8. Wang, J.; Guo, G. X.; Li, A. M.; Cai, W. Q.; Wang, X. W. *Exp Ther Med* **2021**, 21, (3).
9. Vitek, L. *Med Res Rev* **2020**, 40, (4), 1335-1351.
10. Zietz, B.; Gillbro, T. *J. Phys. Chem. B* **2007**, 111, (41), 11997-12003.
11. Zietz, B.; Blomgren, F. *Chem. Phys. Lett.* **2006**, 420, (4-6), 556-561.
12. Zietz, B.; Macphersona, A. N.; Gillbro, T. *Phys. Chem. Chem. Phys.* **2004**, 6, (19), 4535-4537.
13. Mazzoni, M.; Agati, G.; Troup, G.; Pratesi, R. *J. Opt. A-Pure Appl. Op.* **2003**, 5, (5), S374.
14. Sloper, R.; Truscott, T. *Photochem. and Photobio.* **1980**, 31, (5), 445-450.
15. Petersen, C. E.; Ha, C. E.; Harohalli, K.; Feix, J. B.; Bhagavan, N. V. *J. Bio. Chem.* **2000**, 275, (28), 20985-20995.
16. Sato, H.; Honore, B.; Brodersen, R. *Arch Biochem Biophys* **1988**, 260, (2), 811-821.
17. Ziberna, L.; Martelanc, M.; Franko, M.; Passamonti, S. *Scientific Reports* **2016**, 6.
18. Weisiger, R. A.; Ostrow, J. D.; Koehler, R. K.; Webster, C. C.; Mukerjee, P.; Pascolo, L.; Tiribelli, C. *J. Bio. Chem.* **2001**, 276, (32), 29953-29960.
19. Madea, D.; Mahvidi, S.; Chalupa, D.; Mujawar, T.; Dvořák, A.; Muchová, L.; Janoš, J. i.; Slavicek, P.; Švenda, J.; Vitek, L. *J. T. J. o. O. C.* **2020**, 85, (20), 13015-13028.
20. Lamola, A. A., *Optical Properties and Structure of Tetrapyrroles*. W. de Gruyter: Berlin, 1985.
21. Rohmer, T.; Matysik, J.; Mark, F. *J. Phys. Chem. A* **2011**, 115, (42), 11696-11714.
22. Bonnett, R.; Davies, J.; Hursthouse, M.; Sheldrick, G. J. P. o. t. R. S. o. L. S. B. B. S. **1978**, 202, (1147), 249-268.
23. Chen, Y. H.; Li, N. X.; Wang, L. G.; Li, L.; Xu, Z. Q.; Jiao, H. Y.; Liu, P. F.; Zhu, C.; Zai, H. C.; Sun, M. Z.; Zou, W.; Zhang, S.; Xing, G. C.; Liu, X. F.; Wang, J. P.; Li, D. D.; Huang, B. L.; Chen, Q.; Zhou, H. P. *Nat. Commun.* **2019**, 10.
24. El-Zohry, A. M.; Shaheen, B. S.; Burlakov, V. M.; Yin, J.; Hedhili, M. N.; Shikin, S.; Ooi, B.; Bakr, O. M.; Mohammed, O. F. *Chem* **2019**, 5, (3), 497-499.
25. Moglich, A.; Joder, K.; Kiefhaber, T. *PNAS* **2006**, 103, (33), 12394-12399.
26. Liu, D.; El-Zohry, A. M.; Taddei, M.; Matt, C.; Bussotti, L.; Wang, Z.; Zhao, J.; Mohammed, O. F.; Donato, M. D.; Weber, S. *Angew. Chem. Int. Edit.* **2020**, n/a, (n/a), 11591-11599.
27. Imran, M.; El-Zohry, A. M.; Matt, C.; Taddei, M.; Doria, S.; Bussotti, L.; Foggi, P.; Zhao, J.; Di Donato, M.; Mohammed, O. F.; Weber, S. *Journal of Materials Chemistry C* **2020**, 8, (24), 8305-8319.
28. Hussain, M.; El-Zohry, A. M.; Gobeze, H. B.; Zhao, J. Z.; D'Souza, F.; Mohammed, O. F. *J. Phys. Chem. A* **2018**, 122, (29), 6081-6088.
29. Lamola, A. A.; Flores, J. *J. Am. Chem. Soc.* **1982**, 104, (9), 2530-2534.
30. El-Zohry, A. M.; Zietz, B. *J. Phys. Chem. C* **2013**, 117, (13), 6544-6553.
31. El-Zohry, A. M. *Dyes Pigm.* **2019**, 160, 671-674.
32. El-Zohry, A. M.; Alturki, A.; Yin, J.; Mallick, A.; Shekhah, O.; Eddaoudi, M.; Ooi, B. S.; Mohammed, O. F. *J. Phys. Chem. C* **2019**, 123, (10), 5900-5906.
33. El-Zohry, A. M.; Karlsson, M. *J. Phys. Chem. C* **2018**, 122, (42), 23998-24003.
34. El-Zohry, A. M.; Roca-Sanjuan, D.; Zietz, B. *J. Phys. Chem. C* **2015**, 119, (5), 2249-2259.
35. Abdelhamid, H. N.; El-Zohry, A. M.; Cong, J.; Thersleff, T.; Karlsson, M.; Kloo, L.; Zou, X. *Royal Society open science* **2019**, 6, (7), 190723.
36. El-Zohry, A. M.; Orthaber, A.; Zietz, B. *J. Phys. Chem. C* **2012**, 116, (50), 26144-26153.

37. Sirbu, D.; Karlsson, J. K. G.; Harriman, A. *J. Phys. Chem. A* **2018**, 122, (47), 9160-9170.
38. Shirakov, A.; Burshtein, Z.; Katzir, A.; Frumker, E.; Ishaaya, A. A. *Opt Express* **2018**, 26, (9), 11694-11707.
39. Itoh, S.; Okada, H.; Kuboi, T.; Kusaka, T. *Pediatr Int* **2017**, 59, (9), 959-966.
40. Ebbesen, F.; Madsen, P. H.; Vandborg, P. K.; Jakobsen, L. H.; Trydal, T.; Vreman, H. *J. Pediatric Research* **2016**, 80, (4), 511-515.
41. Zietz, B.; Blomgren, F. *Chem. Phys. Lett.* **2006**, 420, 556-561.
42. Zietz, B.; Macpherson, A. N.; Gillbro, T. *Phys. Chem. Chem. Phys.* **2004**, 6, 4535-4537.